Published in final edited form as:
Biomaterials. 2012 January ; 33(2): 535–544. doi:10.1016/j.biomaterials.2011.09.079.

Engineering fibrin polymers through engagement of alternative polymerization mechanisms

Sarah E. Stabenfeldt[a], **Merek Gourley**[a], **Laxminarayanan Krishnan**[b], **James B. Hoying**[b], and **Thomas H. Barker**[a,*]

[a]Wallace H. Coulter Department of Biomedical Engineering, Georgia Institute of Technology/ Emory University, 313 Ferst Dr., Atlanta, GA 30332, USA

[b]Division of Cardiovascular Therapeutics, Cardiovascular Innovation Institute, University of Louisville, Louisville, KY, USA

Abstract

Fibrin is an attractive material for regenerative medicine applications. It not only forms a polymer but also contains cryptic matrikines that are released upon its activation/degradation and enhance the regenerative process. Despite this advantageous biology associated with fibrin, commercially available systems (e.g. TISSEEL) display limited regenerative capacity. This limitation is in part due to formulations that are optimized for tissue sealant applications and result in dense fibrous networks that limit cell infiltration. Recent evidence suggests that polymerization knob ‘B’ engagement of polymerization hole ‘b’ activates an alternative polymerization mechanism in fibrin, which may result in altered single fiber mechanical properties. We hypothesized that augmenting fibrin polymerization through the addition of PEGylated knob peptides with specificity to hole ‘b’ (AHRPYAAC-PEG) would result in distinct fibrin polymer architectures with grossly different physical properties. Polymerization dynamics, polymer architecture, diffusivity, viscoelasticity, and degradation dynamics were analyzed. Results indicate that specific engagement of hole ‘b’ with PEGylated knob ‘B’ conjugates during polymerization significantly enhances the porosity of and subsequent diffusivity through fibrin polymers. Paradoxically, these polymers also display increased viscoelastic properties and decreased susceptibility to degradation. As a result, fibrin polymer strength was significantly augmented without any adverse effects on angiogenesis within the modified polymers.

Keywords

Fibrin; Angiogenesis; Mechanical properties; Biodegradation

1. Introduction

Biologically derived polymeric hydrogels are attractive materials for regenerative medicine as degradation/remodeling may occur via inherent proteolytic mechanisms. A range of biological materials have been investigated as the basis for regenerative hydrogels including fibrin, collagen, basement membrane composite blend (Matrigel), and protein-synthetic hybrid molecules (See Refs. [1,2]). Unlike most synthetic materials, these materials possess inherent cell responsive elements that mediate cell–protein interactions (i.e. integrin-ECM interactions), proteolytic degradation, and remodeling. One drawback of biologically

*Corresponding author. Tel.: +1 404 385 5039; fax: +1 404 894 4243. thomas.barker@bme.gatech.edu (T.H. Barker).

derived materials is limited control over mechanical and physical properties due to the complex and potentially unknown protein–protein interactions central to their polymerization. However, new methods to tune bulk and macroscopic properties of biological polymers may emerge if more knowledge is acquired about the polymerization mechanisms at the molecular level.

Fibrin is one such biological material that has been well studied and in turn heavily utilized for commercial products (e.g. TISSEEL, Evicel). In physiological settings, fibrin is at the crux of the coagulation cascade whereby an intricate series of enzymatic signaling converts soluble plasma protein fibrinogen to fibrin in an effort to prevent blood loss and maintain hemostasis. Commercial fibrin products use high concentrations of fibrinogen and thrombin, at least one order of magnitude greater than physiological concentrations (30–100 mg/mL vs. 3.3 mg/mL), to generate a matrix with enhanced initial mechanical stability. However, highly concentrated fibrinogen/thrombin formulations significantly increase polymerization rates necessitating specialized applicators for delivery. Moreover, the resulting dense fibrin network is not optimal for cellular infiltration [3]. Therefore, there is an obvious need to control the final macroscopic properties of the fibrin matrix to enhance cell infiltration and matrix degradation while maintaining mechanical integrity, thus shifting to a more regenerative paradigm as opposed to scar formation.

Looking at the molecular events during fibrin polymerization, thrombin binds to fibrinogen at the centrally located amino-terminus and cleaves a portion of the Aα-chains known as fibrinopeptide A, thus exposing fibrin knobs ‘A’. These knob domains are then free to interact with neighboring fibrin/fibrinogen monomers at the carboxyl-termini of the γ- and β-chains referred to as the polymerization holes ‘a’ and ‘b’, respectively. Knob ‘A’:hole ‘a’ (A:a) interactions initiate fibrin monomer assembly in an end-to-end orientation forming fibrin protofibrils and account for the majority the knob:hole non-covalent bond strength [4,5]. Thrombin also cleaves a portion of the β-chain N-termini releasing fibrinopeptides B and exposing the knobs ‘B’ at a slower rate than knobs ‘A’. The role of knob ‘B’ is somewhat elusive and is thought to help promote lateral aggregation of protofibrils to form fibrin fibers [6] or stabilize A:a interactions within protofibrils [7]. Recent studies suggest that the release of fibrinopeptides B may facilitate association of the C-termini of Aα chains, so-called αC–αC interactions [8]. This additional αC–αC association between fibrin molecules within fibers is thought to enhance the extensibility of fibrin fibers (see Refs. [9,10]). The fibrin network is further stabilized through covalent crosslinking by the transglutaminase factor XIII (FXIII) between the γ chains and αC chains of adjacent fibrin monomers.

A multitude of parameters influence fibrin polymerization rates and resulting fiber structure including ionic strength, protein and zyomogen concentrations, calcium concentration, and pH [11,12]. In addition to these parameters, synthetic fibrin knob peptide mimics alter fibrin assembly via competition with native fibrin knobs for polymerization hole domains. At high concentrations (>100-fold molar excess), fibrin knob ‘A’ peptide derivatives inhibit fibrin polymerization [13,14]. In contrast, supplementing fibrin clots with synthetic knob ‘B’ peptides has been shown to generate coarser fibrin clots [15,16]. Bovine knob ‘B’ peptide mimic (Gly-His-Arg-Pro-Tyr; GHRPY) has been shown to alter the molecular packing of fibrin molecules such that adjacent fibrin molecules are oriented in a symmetrical anti-parallel manner creating a stable β–β interface [16]. This altered molecular packing orientation with XHRPY peptides delays endogenous tissue plasminogen activator (tPA) and plasminogen mediated fibrinolysis of clots suggesting diminished activity of tPA or disruptions in the plasminogen binding site on fibrin [16]. In summary, perturbation of the either the A:a or particularly B:b interactions significantly influences the dynamics of fibrin monomer and fiber assembly; however, a comprehensive evaluation of how altering the

dynamics of A:a or B:b interactions may influence the end macroscopic physical properties of fibrin gels has not yet been investigated.

Therefore, in this study, we aimed to exploit the inherent biology of fibrin polymerization in order to finely tune the final bulk characteristics of fibrin gels. To achieve this goal, we employed fibrin knob peptide mimics to perturb A:a or B:b interactions at the molecular level and then evaluated the resulting fibrin gel structural, mechanical, and degradation properties. We chose to use the knob 'A' peptide mimic GPRPFPAC since it has been shown to have superior binding affinity compared the tetrapeptide GPRP [17]. For the knob 'B' peptide, we chose the peptide AHRPYAAC since AHRP has been shown to bind only to the polymerization hole 'b' and not hole 'a' while the Tyr5 residue contributes to altered β–β interactions [18]. All peptides used in this study were conjugated to 5 kDa polyethylene (PEG) linear polymer since PEGylation has been shown to increase the activity of the fibrin knob peptides [19]. Moreover, we emphasize that all experiments were performed at equimolar ratios of knob peptide conjugate to fibrinogen inferring that only one knob peptide conjugate was present for every one set of fibrin polymerization holes. At this low ratio, fibrin polymerization is not inhibited, but rather knob:hole interactions are exogenously "pre-engaged" prior to fibrin polymerization. This study concludes with investigating the angiogenic potential of the differing fibrin networks using a microvascular fragment model.

2. Materials and methods

2.1. Polyethylene glycol (PEG)–peptide conjugates

All peptides were synthesized with a cysteine residue at the carboxyl terminus to facilitate PEGylation via maleimide-sulfhydryl chemistry (GPRPFPAC, GPSPFPAC, and AHRPYAAC; GenScript USA Inc, Piscataway, NJ). Briefly, linear maleimide monofunctional PEG monomers capped with a methoxyl group (5 kDa; JenKem Technology USA, Allen, TX) were reconstituted in 100 mM phosphate buffer pH 7.2, 150 mM sodium chloride, 10 mM EDTA solution. The mal-PEG solution was then added to the desired peptide solution at a 1:2 molar ratio (GPSPFPAC, GPRPFPAC, or AHRPYAAC) in phosphate buffer and agitated at 400 rpm for 4 h at room temperature. The resulting PEG-peptide conjugates were dialyzed (2000 MWCO, Slidalyzer, Thermo Fisher) against ultrapure deionized water (dH_2O) to remove unconjugated peptides. Samples were then lyophilized and stored at −20 °C until reconstituted in dH_2O prior to use. Conjugate concentrations were determined through both PEG and protein quantification assays. To determine the concentration of PEG in the samples, previously established iodine assay was performed; non-reacted m-PEG was used for the standard curve [20]. A FluoroProfile® Protein Assay (Sigma–Aldrich, Saint Louis, MO) was completed to determine the concentration of peptide in the sample.

2.2. Thrombin initiated fibrin polymerization assays

All *in vitro* fibrin polymerization assays were conducted with materials purchased from Enzyme Research Laboratories, Inc (South Bend, IN) unless stated otherwise. Purified human fibrinogen (FIB3; plasminogen, von Willebrand factor, and fibronectin depleted) was mixed with human α-thrombin and activated factor XIII (FXIIIa) to initiate clot formation with final working concentrations of 1 or 4 mg/ml fibrinogen, 1 U/mL thrombin, and 1 U/mL FXIIIa diluted in 137.5 mM Tris–HCl + 50 mM NaCl and 5 mM $CaCl_2$ (TSBC). For experimental conditions, fibrinogen was pretreated with three synthetic, PEGylated peptides (GPSPFPAC-PEG, GPRPFPAC-PEG, and AHRPYAAC-PEG) for 30 min at a 1:1 molar ratio prior to thrombin-initiated clotting. Clotting assays were performed in flat transparent

optical 96-well plates (end working volume: 100 μL). Turbidity and percent clottable protein were used to measure alterations in clotting.

Turbidity experiments were performed to monitor fibrin polymerization rates and end turbidity values. Control and experimental groups of fibrinogen were prepared as described above. Immediately after mixing the thrombin and FXIIIa solution with fibrinogen, the absorbance at 350 nm was recorded every minute for 60 min (350 nm; SpectraMax M2 Microplate Reader, Molecular Devices, Sunnyvale, CA). At least three triplicate trials were performed for each group.

Fibrin clots were prepared as described above and allowed to polymerize for 1 h at which point the non-soluble clot was removed with a pipette tip. The protein concentration of the remaining soluble protein solution (clot liquor) was measured with Quant-iT Protein Assay (Invitrogen; Carlsbad, CA). Percent clottable protein was reported as the initial soluble protein minus the soluble protein in the clot liquor divided by the initial soluble protein. At least three triplicate trials were performed for each group.

2.3. Microstructural analysis

The microstructure of fibrin clots were evaluated with confocal microscopy. Fibrinogen was fluorescently labeled with Alexa-555 nm *N*-hydroxysuccinimide reactive fluorophore (Invitrogen). Fibrin clots (control and experimental groups) containing 10% (w/w) labeled fibrinogen were polymerized in the presence of thrombin and FXIIIa in between a glass slide and coverglass. Clots were imaged 1 h after thrombin-initiated polymerization via a Zeiss Laser Scanning Microscope (LSM 510 VIS, Zeiss, Inc., Thornwood, NY). For each image, 3 random 10 μm z-stacks were acquired per gel and analyzed with Zen image analysis software (Zeiss). For each group, 3–5 gels were analyzed.

The architectural properties of the modified clots were also analyzed with scanning electron microscopy (SEM). The pretreated fibrinogen was incorporated into a 200 μL fibrin gel with 1 mg/mL fibrinogen and 1 U/mL thrombin and FXIIIa. Fibrin gels were polymerized for 2 h at which point they were rinsed with HEPES buffer solution and incubated with 2% gluteraldehyde overnight at room temperature. Following fixation, the gels were exposed to an ethanol dehydration gradient (10, 20, 40, 70, 90, 100, and 100% ethanol for 15 min at each concentration) and critical point dried (EMS 850 Critical Point Dryer; Electron Microscopy Sciences, Hatfield, PA). Dehydrated samples were mounted on aluminum stubs and sputter coated with gold-palladium (SC7640 High Resolution Sputter Coater; Quorum Technologies, Ashford, Kent, UK). SEM images were acquired with a Zeiss Ultra60 SEM (Zeiss, Inc.) at 10,000×, 50,000× and 100,000× magnification.

2.4. Diffusion analysis

Solute diffusion through fibrin clots was analyzed using previously characterized microfluidic devices [21]. The device consisted of three large channels and four gel-filled compartments. The central channel flanked on each side by two gel-filled compartments with subsequent channels on the other side. Microfluidic devices were manufactured from polydimethylsiloxane (PDMS, Sylgard 120; Ellsworth Adhesives, Germantown, WI) using a photolithography micropatterned mold. The PDMS devices were covalently attached to a glass slide after plasma oxidation treatment of both surfaces. Upon device assembly, poly-D-lysine (1 mg/mL PDL; Sigma Aldrich) was injected into the microchannels to render the channels hydrophilic. Fibrinogen (control or experimental treatment groups) was mixed with thrombin and FXIIIa, injected into the gel compartments (~5 μL per compartment), and allowed to polymerize for 1 h in a humid chamber. The outer larger micro-channels were filled with 40 kDa Texas Red-conjugated dextran solution (20 ng/mL in TBSC; Invitrogen),

while the central channel was filled with TBSC solution. The diffusion gradient was measured with fluorescent microscopy; images were acquired every 15 min for 6 h. The resulting images were analyzed in ImageJ (NIH). A custom MATLABreg (MathWorks, Natick, MA) analysis code was used to determine the effective diffusion coefficients for each fibrin gel. Three trials of duplicates were performed for each group.

2.5. Fibrinolysis

Fibrinolysis was evaluated with two plasmin degradation assays, (1) exogenous fibrinolysis via plasmin overlay and (2) tissue plasminogen activator (tPA) induced fibrinolysis (endogenous fibrinolysis).

Exogenous Fibrinolysis – Fibrin clots (100 μL of control and experimental treated clots) were polymerized according methods outlined above. After an hour of polymerization, 100 μL of plasmin (0.5 U/mL) was overlaid on top of the fibrin clots and gently agitated at room temperature for 4 h. At specified times, turbidity measurements (350 nm) were recorded and 5 μL samples from the clot liquor were taken to determine protein concentrations with the Quant-iT protein assay. Three triplicate trials were performed for each group.

Endogenous Fibrinolysis – Purified human fibrinogen (4 mg/mL) supplemented with human plasminogen (10.8 μg/mL) was mixed with thrombin (1 U/mL), FXIIIa (0.5 U/mL), and tPA (0.29 μg/mL) to initiate clot formation. For experimental conditions, fibrinogen was pretreated with three different PEGylated peptides (GPSPFPAC-PEG, GPRPFPAC-PEG, and AHRPYAAC-PEG) for 30 min at a 1:1 molar ratio prior to thrombin-initiated clotting. Assays were performed in transparent 96-well plates with final clot volume of 100 μL. Immediately upon initiating polymerization, turbidity measurements were recorded every minute for 1 h. Post-assay analysis included calculating half-lysis time (time at which turbidity decreased to half the maximum absorbance) and half-lysis ratio (half-lysis time normalized to no peptide control). At least three triplicate trials were performed for each group.

2.6. Viscoelasticity analysis

The viscoelastic properties of fibrin clots were measured with an oscillating rheometer (Bohlin CVO 120; Bohlin Instruments, Ltd., East Brunswick, NJ) with a 12 mm parallel plate configuration. The fibrinogen solution with or without PEGylated peptides was mixed with a thrombin and FXIIIa solution and immediately pipetted onto the stage (4 mg/mL fibrinogen,1 U/mL thrombin,1 U/mL FXIIIa). Fibrin clots were allowed to polymerize for 1 h prior to measurements. Samples were subjected to a frequency sweep (0.1 Hz–10 Hz) under constant strain (0.1%) to determine viscoelastic moduli (storage moduli, G'; loss moduli, G''; complex moduli, G*). At least 4 trials were performed for each group.

2.7. Microvessel construct model

Microvessel fragments were isolated from the epididymal adipose tissue of male Sprague–Dawley rats by mincing, followed by limited digestion with collagenase (Worthington Biochemicals, Lakewood, NJ), and sequential filtration through a 500 μm and a 20 μm nylon membrane [22]. Large tissue debris was sequestered on the 500 μm membrane while the 20 μm membrane allowed the smaller fragments and single cells to pass through while retaining only larger microvessel fragments of interest. These fragments, when cultured *in vitro*, in a 3-D collagen type 1 matrix, undergo spontaneous sprouting angiogenesis and progress to form a dense interconnected network [23] that is perfusion capable when implanted *in vivo* [24].

Adipose derived microvessel fragments were suspended at a concentration of 20,000 fragments/mL, in the fibrinogen solutions (same as mentioned in methods above) already incubating for 15 min, and immediately mixed with appropriate volumes of thrombin and cast into a 3-D gel in tissue culture plates. Gels were allowed to polymerize for 1 h and covered with 10% FBS and aprotinin containing media. Typical leaf-like outgrowths from the parent fragments begin to appear by the 4th day in culture and are referred to as neovessel sprouts. The sprouts gradually fill up the construct space and form an interconnected network pattern by the 10th day [22,23]. Media was changed on the 4th day and every second day subsequently.

2.8. Microscopy and image analysis of microvessel cultures

Cultures were fixed on the 10th day with 2% para-formaldehyde, permeabilized with 0.1% Triton X, and stained with FITC conjugated GS-1 (Vector Labs, Burlingame, CA) to label the microvessel networks. Images were acquired using both a 4× and a 10× objective from 5 random areas of each construct. A total of 3 constructs were examined for each of the 4 test conditions. Florescence microscopy images recorded with the 4× objective were deconvolved, thresholded, binarized and size-filtered using a custom routine in Matlab (Mathworks, Natick, MA). The binarized images were then imported into Amira (Visage Imaging, San Diego, CA) to extract the medial skeleton and local diameter information as described earlier [25]. This data was further processed in WinFiber3D (http://mrl.sci.utah.edu/software/winfiber3d; [25]), a custom analysis software, to parse morphological information like lengths and diameters from the medial skeleton. In the subsequent analysis, a node was defined as a point where the microvessel, represented now by its medial skeleton, either branched or terminated. The region between such nodes was designated as a segment. A complete series of such connected segments was defined as a network. Thus the mean segment length is indicative of how long each segment grows before it either terminates or branches while the total number of networks and total length of networks indicate the total ‘vascularity’ of the construct.

2.9. Statistical analysis

Data are presented as the mean ± one standard deviation. Results were analyzed by the appropriate one- or two-way ANOVA, followed by pair-wise comparisons with Tukey’s or Bonferroni’s post-hoc test (Prism 5, GraphPad Software, Inc., La Jolla, CA). For microvessel assays, multiple 1-way ANOVAs or their non-parametric equivalents (Systat Software Inc, San Jose, CA) were used to compare the effect of treatment on the number of networks, mean network length, total network length, segment lengths as well as segment diameters. A 95% confidence level and corresponding p value <0.05 was considered significant.

3. Results

3.1. Fibrin polymerization and percent clottability

At high concentrations (i.e.100-fold molar excess) fibrin knob ‘A’ peptides have been shown inhibit fibrin polymerization [13,14]. Using PEGylated knob peptides at a 1:1 molar ratio with fibrinogen, we aimed to alter the polymerization dynamics but not inhibit fibrin clot formation. For the turbidity assay at 1 mg/mL fibrinogen (Fig. 1A), equimolar supplement of the knob ‘A’ conjugate (GPRPFPAC-PEG) did not significantly alter the turbidity curve compared to no peptide control and control peptide conjugate (GPSPFPAC-PEG). However, the addition of knob ‘B’ conjugate (AHRYPAAC-PEG) significantly increased the absorbance consistently throughout polymerization. Interestingly, for the 4 mg/mL fibrin clot, the knob ‘B’ conjugate resulted in a significant increase in absorbance only during the lag and reaction phases of polymerization, but the final peak absorbance

value was not significantly different from controls (Fig. 1B). No significant difference was observed with the equimolar supplement of knob ‘A’ conjugate at 4 mg/mL (Fig. 1B).

In the presence of knob ‘A’ or knob ‘B’ conjugate, a modest yet significant decrease in the percent clottable protein (92% and 93% respectively) was observed compared to controls (95%; $p < 0.01$; Fig. 1C). However, neither knob peptide conjugate reduced the percent clottable protein below 90%, a lower limit specified for a formidable fibrin clot. Collectively, these results demonstrated that at equimolar ratios, formidable fibrin gels polymerized in the presence of knob peptide conjugates; however, variations in peak absorbance turbidity values suggest structural alterations among each group.

3.2. Structural analysis

The microarchitecture and fiber structure of the resulting fibrin gels were evaluated in hydrated (confocal microscopy) and dehydrated (SEM) states (Fig. 2). Representative confocal microscopy demonstrated stark differences in fiber density and size in addition to network organization (Fig. 2). Notably, equimolar addition of knob ‘A’ (GPRPFPAC-PEG; Fig. 2C) and knob ‘B’ (AHRPYAAC-PEG; Fig. 2D) conjugates resulted in more porous fibrin networks compared to control groups (no peptide and GPSPFPAC-PEG; Fig. 2A and B). Comparing the knob conjugates directly highlights the critical A:a interaction during fibrin assembly as the fibers appeared thinner in the knob ‘A’ conjugate group compared to the knob ‘B’ conjugate group. SEM analysis enabled a more in depth evaluation of the fiber structure/size. The representative SEM micrographs supported the confocal data as the network organization of both knob ‘A’ and knob ‘B’ conjugates groups (Fig. 2G and H, respectively) appeared less dense and more porous compared to no peptide and knob peptide control groups (Fig. 2E and F, respectively). Moreover, the knob ‘A’ conjugate treated fibrin gels appeared to have the thinnest fibers and an increased occurrence of truncated fibers. Engaging polymerization hole ‘b’ with the knob ‘B’ conjugates generated fibrin fibers that appeared to have greater distance between branching points. Collectively, these results illustrate how modifying molecular interactions during fibrin polymerization will markedly affect the final fibrin structure.

3.3. Effective diffusion

The effective diffusion coefficient for each of the 4 mg/mL fibrin gel formulations was measured by visually tracking the diffusion of a fluorescently labeled dextran (Fig. 3A). The results indicated that effective diffusion coefficient for the either knob conjugates (GPRPFPAC-PEG and AHRPYAAC-PEG) resulted in a significant 50–70% increase in effective diffusion coefficient compared to the control gels (no peptide and GPSPFPAC-PEG; Fig. 3B; $p < 0.001$). Comparing the two knob conjugates directly revealed that the effective diffusion coefficient for knob ‘A’ (GPRPFPAC-PEG) was significantly greater than knob ‘B’ (AHRPYAAC-PEG; $p < 0.01$). Collectively, this observed increase in effective diffusion coefficient further validates the SEM and confocal images that revealed the highest porosity within the knob ‘A’ conjugate treated fibrin gels (knob ‘A’ > knob ‘B’ > control peptide ~ no peptide control).

3.4. Fibrinolysis

Fibrinolysis or degradation of the fibrin clot through enzymatic plasmin degradation was investigated via exogenous and endogenous activation. The exogenous plasmin degradation assay evaluates fibrinolysis of a pre-formed clot whereby active plasmin was overlaid on top of a stable clot and is independent of plasmin activation. Degradation was monitored with turbidity readings and measuring the soluble protein levels over the course of the assay. The results indicated that with 1 mg/mL fibrin gels, an enhanced turbidity reading was observed with the knob ‘B’ conjugate (AHRPYAAC-PEG) at 0 and 60 min (Fig. 4A); however, no

difference in percent soluble protein was observed among any of the groups (Fig. 4B). In contrast, at 4 mg/mL fibrin gels, significantly higher turbidity readings were observed with the knob 'B' conjugate only at the latter time points (Fig. 4C). Similar to the 1 mg/mL fibrin gels, no significant differences in soluble proteins levels were observed among the groups (Fig. 4D). We found these results somewhat surprising as exogenous fibrinolysis (i.e. the addition of preactivated plasmin after fibrin polymerization) has been shown to be a diffusion dependent phenomenon [26,27]. Based on structural and diffusion analyses, knob 'A' and knob 'B' conjugates resulted in more porous fibrin networks with nearly doubled effective diffusion coefficients over the control groups. If exogenous fibrinolysis is solely diffusion dependent, then we anticipated that the knob 'A' and knob 'B' fibrin gels would degrade at a much faster rate than the controls. However, the degradation profiles were similar, therefore we speculate that lysis may be mediated by both diffusion limits and the susceptibility of fibrinolysis based on conformational alterations of the fibrin fibers. Therefore, the diffusion into the knob conjugate fibrin gels occurs at a faster rate, but plasmin binding and lysis actually occurs at a slower rate.

The endogenous plasmin degradation assay evaluated fibrinolysis via fibrin-stimulated activation of plasminogen by tissue plasminogen activator (tPA) thus mimicking the endogenous plasmin-mediated fibrinolytic process. Turbidity measurements of the polymerization and subsequent fibrinolysis of 1 mg/mL fibrin gels demonstrated an increased peak absorbance and delayed onset of lysis with knob 'B' conjugate (AHRPYAAC-PEG; Fig. 5A). Surprisingly, at 4 mg/mL fibrin, only fibrinolysis was significantly delayed in the knob 'B' conjugate samples compared to the controls and knob 'A' (GPRPFPAC-PEG) samples, while the peak absorbance was similar among all groups (Fig. 5B). Looking particularly at the half-lysis ratio (time required to reach half the peak absorbance normalized to the no peptide control), a significant increase was observed with the knob 'B' group in the 1 mg/mL fibrin gel (Fig. 5C). In the 4 mg/ml fibrin gels, knob 'B' group again demonstrated a significant increase in half-lysis. Our results match previous reports in which knob 'B' peptides delay tPA-induced fibrinolysis, suggesting diminished activity of the tPA or plasminogen binding site [15,16]. Knob 'B' peptides mimicking bovine fibrin (Gly-His-Arg-Pro-Tyr; GHRPY) have been shown to alter the molecular packing of fibrin molecules such that adjacent fibrin molecules are oriented in a symmetrical anti-parallel manner creating a stable β–β interface mediated by the Tyr5 interacting with a glutamine on neighboring β-chains [16]. The B:b interaction also perturbs a stable calcium bridge between the βC-domain and the coiled coil domain initiating the βC domain to swing out and enhance the propensity for β–β interactions. This model further hypothesizes that B:b interactions may strengthen intra-fibril interactions [10,28]. Therefore, variations either in fibrin monomer packing or β–β interactions via 'pre'-engagement of B:b interactions may result in diminished tPA and plasminogen binding and/or susceptibility to plasmin degradation.

3.5. Viscoelasticity

Viscoelastic studies were performed with a stress-controlled rheometer under a low frequency sweep with amplitude strain. Fibrin gels supplemented with equimolar ratio of knob 'A' conjugate (GPRPFPAC-PEG) resulted in a significant 30% decrease in complex moduli as compared to controls (no peptide and GPSPFPAC-PEG, Fig. 6). This result was not surprising as the knob 'A' conjugates predominately engages polymerization hole 'a', in which native A:a interactions have been shown dominate fibrin assembly and accounts for the majority of strength between fibrin monomer–monomer non-covalent interactions. Therefore, by using knob 'A' conjugates, we were essentially inhibiting the strongest interaction, which had a detrimental effect on the viscoelastic properties. Moreover, looking at the SEM images, we also observed truncated fibers that may indicate the knob 'A'

conjugates capped and terminated protofibril growth, thus further impacting bulk mechanical properties of the fibrin gels. In stark contrast, engaging the B:b interaction with the knob 'B' conjugates significantly enhanced the complex moduli over the controls by nearly 35–40%. Looking at the network structure via SEM and confocal, we observed more porous and less dense fiber networks compared controls. Therefore, this increase in mechanical properties was somewhat surprising since, from a mechanical stand point, less dense networks composed of the same material typically translates to a decrease in mechanical properties. Therefore, we hypothesize that the knob 'B' conjugates may be (1) altering fibrin monomer packing, (2) increase β–β interactions, and/or (3) increasing αC–αC interactions that in turn significantly strengthen the bulk mechanical properties of the fibrin gel. Collectively, these results demonstrated significant mechanical alterations of the fibrin gels that were dependent on the molecular interactions that occurred during polymerization.

3.6. Microvessel construct model

The microvessel fragment assay eloquently models angiogenesis as the isolated parent vessels maintain the extracellular matrix and cellular architecture (both endothelial cells and periocytes) opposed to mono-cell cultures of isolated endothelial cells [22,23]. In this study, we used this unique *in vitro* model to evaluate the angiogenic potential of our fibrin gels. Our results demonstrated that all groups supported angiogenesis and neovessel sprouting by day 10 (Fig. 7A–D); the neovessel growth observed in fibrin gels was comparable to levels of growth previously reported in collagen I gels [25]. We observed a trend in the no peptide, control peptide (GPSPFPAC-PEG), and knob 'B' (AHRPYAAC-PEG) groups towards toward a higher number of networks and total network lengths particularly compared to the knob 'A' group (GPRPFPAC-PEG; Fig. 7E). Looking specifically at neovessel segments, the knob 'A' group was seen to have lower segment length compared to control and knob 'B' groups (Fig. 7F). However, no statistical significance was observed among the groups for any of the quantified measurements. Given the differences in mechanical and structural properties, these results were somewhat surprising and warrant further exploration in subsequent studies.

4. Discussion

In this study, we investigated the effect of exogenously engaging fibrin polymerization holes during fibrin assembly and polymerization on the resulting fibrin network's physical and mechanical outcomes. Effectively, we augmented the fibrin fiber assembly thereby demonstrating a relationship between fibrin monomer assembly and the end macroscopic bulk properties. We specifically focused on pre-engaging either the strong A:a interaction or the weaker B:b interaction. The data suggest that exogenously engaging either polymerization hole 'a' or 'b' resulted in an increased porous fibrin network and thus increased diffusive properties. However, stark differences in the mechanical and fibrinolysis properties were dependent on the knob conjugate. For instance, the knob 'A' conjugate significantly decreased the viscoelasticity nearly 30% of the controls, but did not alter endogenous or exogenous fibrinolysis. In contrast, the knob 'B' conjugate significantly increased the viscoelasticity nearly 40% over the control groups and significantly delayed endogenous fibrinolysis by 15% over the control groups. Despite such absolute changes in the mechanical and structural properties, angiogenesis as measured by neovessel sprouting from microvessels was not significantly different among the control and experimental groups.

The most notable finding in this study was extreme variations in the mechanical properties of fibrin gels. For knob 'A' conjugate samples, the complex moduli decreased by 35% over controls. However, the knob 'B' conjugate significantly enhanced the complex moduli

compared to control fibrin gels. As mentioned previously, the decreased mechanical integrity of fibrin as a result of engaging hole ‘a’ with exogenous knob ‘A’ conjugates was not surprising. The A:a interaction between native fibrin(ogen) monomers instigates initial fibrin monomer assembly into fibrin protofibrils. Moreover, the A:a interaction accounts for majority of the non-covalent bond strength between monomers [5]. The addition of exogenous knob ‘A’ conjugates have the potential to effectively cap fibrin monomers and inhibit polymerization. However, the significant increase in complex moduli with the knob ‘B’ conjugates was surprising. The knob ‘B’ peptide sequence was specifically chosen to avoid potential B:a interactions and solely engage hole ‘b’. With that said, little information is known about the macroscopic consequences of engaging hole ‘b’. During fibrin polymerization under normal physiological conditions, knob ‘A’ is exposed at a much faster rate than knob ‘B’ thus delaying any B:b interactions that may occur. In our study, we pre-incubated fibrinogen with the knob conjugates prior to initiating polymerization. Therefore, B:b interactions were allowed to occur prior to release of the fibrinopeptides B. This raises many questions as to the role of B:b interactions in controlling the dynamics of fibrin assembly. Do conformational changes occur to enhance the propensity for (1) β–β interactions, (2) altered molecular packing, or (3) αC–αC interactions? This study has convincingly demonstrated that these molecular interactions will have an effect on macroscopic properties, but the how and why questions still remain. Our approach of engaging holes ‘b’ prior to thrombin activation of the fibrinogen molecule are a stark contrast to previous reports exploring the role of knobs ‘B’ in fibrin fiber assembly using partially activated fibrin displaying knobs ‘A’ or knobs ‘B’ only on the native molecule.

For the *in vitro* angiogenic study, we used a physiologically relevant fibrinogen concentration of 4 mg/mL (average blood concentration ~3.3 mg/mL), a concentration that is known to support angiogenesis in native wound healing contexts. We observed a trend whereby the knob ‘B’ conjugate group supported network formation and neovessel sprouting to similar levels as the control fibrin gels despite significantly different mechanical properties. However, the knob ‘A’ conjugate had lower total network compared to all other groups, but not statistically significant. Our results demonstrate the cell permissiveness of fibrin gels at 4 mg/mL was not significantly impacted by the mechanical or structural nature of the fibrin network. Comparing our conditions to previous studies using fibrin-based 3-D cell cultures, it should be noted that it is not uncommon to see the use of 8–30 mg/mL fibrin gels [29,30]. Moreover, current fibrin sealants on the market contain even higher concentrations of fibrinogen on the order 50–80 mg/mL. Thus, higher fibrinogen concentrations may accentuate potential variations in cellular response based on structure and mechanical properties of fibrin. In other words, we likely have not deviated outside of the pro-angiogenic range observed with physiologically relevant fibrin concentrations. For future studies, mechanical matching of fibrin groups and/or investigating a broader range of fibrinogen concentrations may provide more insight into cellular response within our modified fibrin gels.

5. Conclusion

Fibrin-based products are naturally derived scaffolds that are appropriate for multiple tissue engineering applications. Here in this study, we developed a method to modify final bulk properties of fibrin gels by engaging theorized alternative polymerization mechanisms. Even at equimolar concentrations, fibrin knob conjugates engage the inherent fibrin monomer and assembly mechanisms to ultimately impact the macroscopic properties. Specifically, fibrin knob ‘A’ conjugates significantly increased porosity and diffusion, but decreased complex moduli and did not affect fibrinolysis. In contrast, fibrin knob ‘B’ conjugates significantly increased porosity, diffusion, and complex moduli in addition to delaying endogenous fibrinolysis. This phenomenon was of particular interest as we effectively discovered a

method to enhance porosity but strengthen a fibrin network. This finding will significantly impact the fibrin-based products, particularly fibrin-sealants, where high mechanical strength is desired to stop hemorrhaging and bind tissues, but cellular infiltration is desired to promote wound healing/regeneration.

Acknowledgments

This work was supported by the NIH (1R01EB011566 and 1R01NS065109; T.H.B.) and the NIH IRACDA Post-doctoral Fellow-ship (K12 GM000680; S.E.S.). The authors acknowledge Drs. Roger Kamm and Ho Seok Park for assistance with microfluidic device preparation, and Allyson Soon and Nader Aboujamous for technical assistance.

References

1. Ahmed TAE, Dare EV, Hincke M. Fibrin: a versatile scaffold for tissue engineering applications. Tissue Eng Pt B-Rev. 2008; 14:199–215.
2. Mano JF, Silva GA, Azevedo HS, Malafaya PB, Sousa RA, Silva SS, et al. Natural origin biodegradable systems in tissue engineering and regenerative medicine:present status and some moving trends. JR Soc Interface. 2007; 4:999–1030.
3. Schmoekel HG, Weber FE, Schense JC, Gratz KW, Schawalder P, Hubbell JA. Bone repair with a form of BMP-2 engineered for incorporation into fibrin cell ingrowth matrices. Biotechnol Bioeng. 2005; 89:253–262. [PubMed: 15619323]
4. Averett LE, Geer CB, Fuierer RR, Akhrernitchev BB, Gorkun OV, Schoenfisch MH. Complexity of “A-a” knob-hole fibrin interaction revealed by atomic force spectroscopy. Langmuir. 2008; 24:4979–4988. [PubMed: 18351791]
5. Litvinov RI, Gorkun OV, Owen SF, Shuman H, Weisel JW. Polymerization of fibrin: specificity, strength, and stability of knob-hole interactions studied at the single-molecule level. Blood. 2005; 106:2944–2951. [PubMed: 15998829]
6. Blomback B, Hessel B, Hogg D, Therkildsen L. A two-step fibrinogen –fibrin transition in blood coagulation. Nature. 1978; 275:501–505. [PubMed: 692730]
7. Okumura N, Terasawa F, Haneishi A, Fujihara N, Hirota-Kawadobora M, Yamauchi K, et al. B:b interactions are essential for polymerization of variant fibrinogens with impaired holes ‘a’. J Thromb Haemost. 2007; 5:2352–2359. [PubMed: 17922804]
8. Litvinov RI, Yakovlev S, Tsurupa G, Gorkun OV, Medved L, Weisel JW. Direct evidence for specific interactions of the fibrinogen alpha C-domains with the central E region and with each other. Biochemistry. 2007; 46:9133–9142. [PubMed: 17630702]
9. Falvo MR, Gorkun OV, Lord ST. The molecular origins of the mechanical properties of fibrin. Biophysical Chem. 2010; 152:15–20.
10. Lord ST. Molecular mechanisms affecting fibrin structure and stability. Arterioscl Throm Vas. 2011; 31:494–499.
11. Carr ME, Gabriel DA, Mcdonagh J. InfluenceofCa-2+ on the structure of reptilase-derived and thrombin-derived fibringels. Biochem J. 1986; 239:513–516. [PubMed: 3548699]
12. Carr ME, Kaminski M, Mcdonagh J, Gabriel DA. Influence of ionic-strength, peptide release and calcium on the structure of reptilase and thrombin derived fibrin gels. Thromb Haemostasis. 1985; 54:159–159.
13. Laudano AP, Doolittle RF. Studies on synthetic peptides that bind to fibrinogen and prevent fibrin polymerization. Structural requirements, number of binding sites, and species differences. Biochemistry. 1980; 19:1013–1019. [PubMed: 7356959]
14. Laudano AP, Doolittle RF. Synthetic peptide derivatives that bind to fibrinogen and prevent the polymerization of fibrin monomers. Proc Natl Acad Sci U S A. 1978; 75:3085–3089. [PubMed: 277910]
15. Doolittle RF, Pandi L. Probing the β-chain hole of fibrinogen with synthetic peptides that differ at their amino termini. Biochemistry. 2007; 46:10033–10038. [PubMed: 17688324]

16. Pandi L, Kollman JM, Lopez-Lira F, Burrows JM, Riley M, Doolittle RF. Two families of synthetic peptides that enhance fibrin turbidity and delay fibrinolysis by different mechanisms. Biochemistry. 2009; 48:7201–7208. [PubMed: 19588915]
17. Stabenfeldt SE, Gossett JJ, Barker TH. Building better fibrin knob mimics: an investigation of synthetic fibrin knob peptide structures in solution and their dynamic binding with fibrinogen/fibrin holes. Blood. 2010; 116:1352–1359. [PubMed: 20484082]
18. Doolittle RF, Chen A, Pandi L. Differences in binding specificity for the homologous gamma- and β-chain "holes" on fibrinogen: exclusive binding of Ala-His-Arg-Pro-amide by the β-chain hole. Biochemistry. 2006; 45:13962–13969. [PubMed: 17115691]
19. Stabenfeldt SE, Aboujamous NM, Soon AS, Barker TH. A new direction for anticoagulants: inhibiting fibrin assembly with PEGylated fibrin knob mimics. Biotechnol Bioeng. 2011
20. Gong XW, Wei DZ, He ML, Xiong YC. Discarded free PEG-based assay for obtaining the modification extent of pegylated proteins. Talanta. 2007; 71:381–384. [PubMed: 19071315]
21. Vickerman V, Blundo J, Chung S, Kamm R. Design, fabrication and implementation of a novel multi-parameter control microfluidic platform for three-dimensional cell culture and real-time imaging. Lab Chip. 2008; 8:1468–1477. [PubMed: 18818801]
22. Hoying JB, Boswell CA, Williams SK. Angiogenic potential of microvessel fragments established in three-dimensional collagen gels. In Vitro Cell Dev Biol Anim. 1996; 32:409–419. [PubMed: 8856341]
23. Krishnan L, Hoying JB, Nguyen H, Song H, Weiss JA. Interaction of angiogenic microvessels with the extracellular matrix. Am J Physiol Heart Circ Physiol. 2007; 293:H3650–H3658. [PubMed: 17933969]
24. Shepherd BR, Chen HY, Smith CM, Gruionu G, Williams SK, Hoying JB. Rapid perfusion and network remodeling in a microvascular construct after implantation. Arterioscler Thromb Vasc Biol. 2004; 24:898–904. [PubMed: 14988090]
25. Krishnan L, Underwood CJ, Maas S, Ellis BJ, Kode TC, Hoying JB, et al. Effect of mechanical boundary conditions on orientation of angiogenic microvessels. Cardiovasc Res. 2008; 78:324–332. [PubMed: 18310100]
26. Veklich Y, Francis CW, White J, Weisel JW. Structural studies of fibrinolysis by electron microscopy. Blood. 1998; 92:4721–4729. [PubMed: 9845538]
27. Sakharov DV, Nagelkerke JF, Rijken DC. Rearrangements of the fibrin network and spatial distribution of fibrinolytic components during plasma clot lysis – study with confocal microscopy. J Biol Chem. 1996; 271:2133–2138. [PubMed: 8567670]
28. Doolittle RF, Pandi L. Binding of synthetic B knobs to fibrinogen changes the character of fibrin and inhibits its ability to activate tissue plasminogen activator and its destruction by plasmin. Biochemistry. 2006; 45:2657–2667. [PubMed: 16489759]
29. Davis HE, Miller SL, Case EM, Leach JK. Supplementation of fibrin gels with sodium chloride enhances physical properties and ensuing osteogenic response. Acta Biomaterialia. 2011; 7:691–699. [PubMed: 20837168]
30. Martino MM, Mochizuki M, Rothenfluh DA, Rempel SA, Hubbell JA, Barker TH. Controlling integrin specificity and stem cell differentiation in 2D and 3D environments through regulation of fibronectin domain stability. Biomaterials. 2009; 30:1089–1097. [PubMed: 19027948]

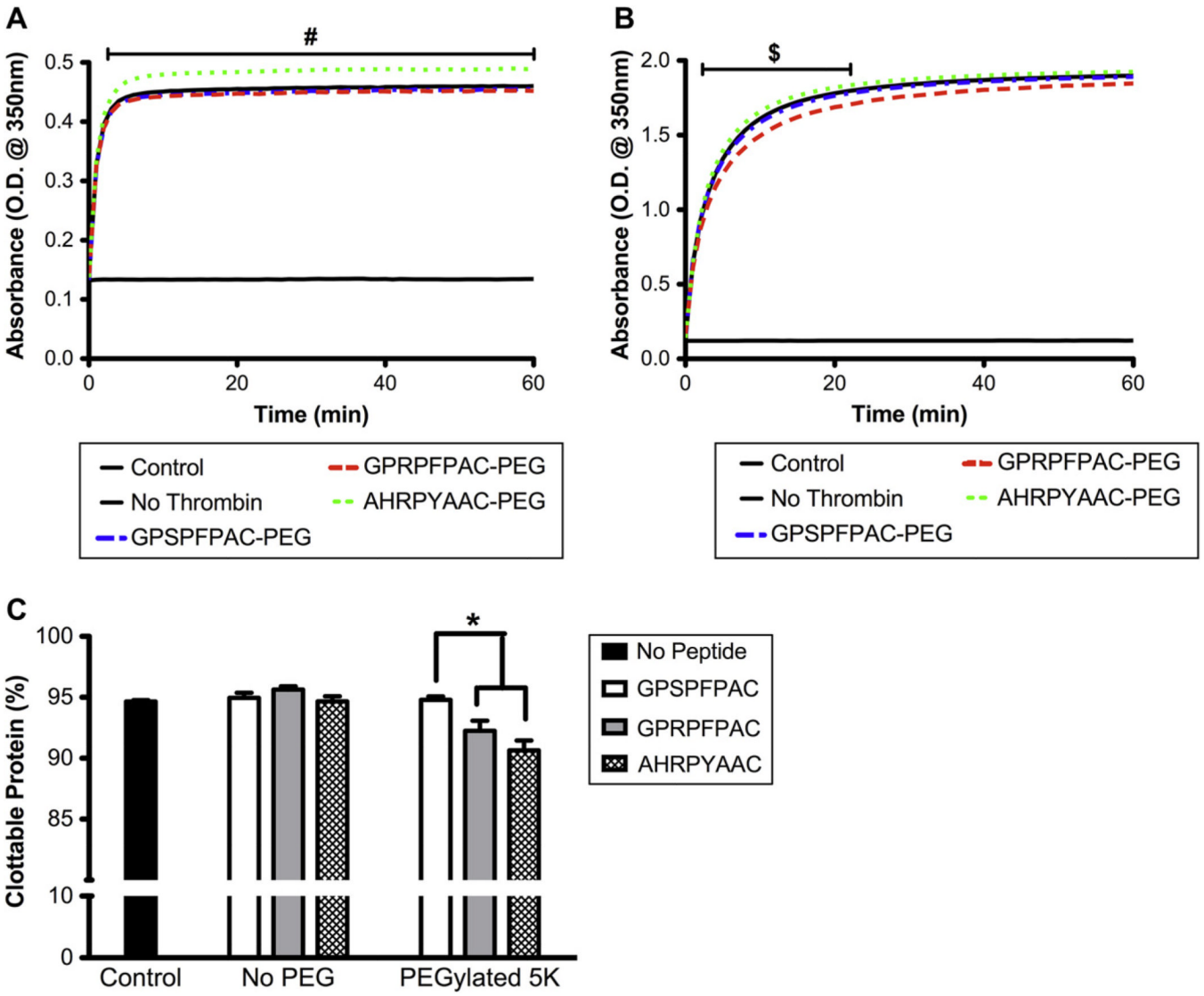

Fig. 1.

Thrombin initiated polymerization: Fibrin polymerization turbidity curves for 1 mg/mL fibrinogen (A) and 4 mg/mL fibrinogen (B). PEGylated peptide conjugates were added at an equimolar ratio to fibrinogen. Percent clottable protein evaluated 60 min after the initiating polymerization for 1 mg/mL fibrinogen gels (C). (Mean ± SD; $n = 6–9$; # denotes $p < 0.01$ relative to all groups, $ denotes $p < 0.01$ relative to GPRPFPAC-PEG, and * denotes $p < 0.01$).

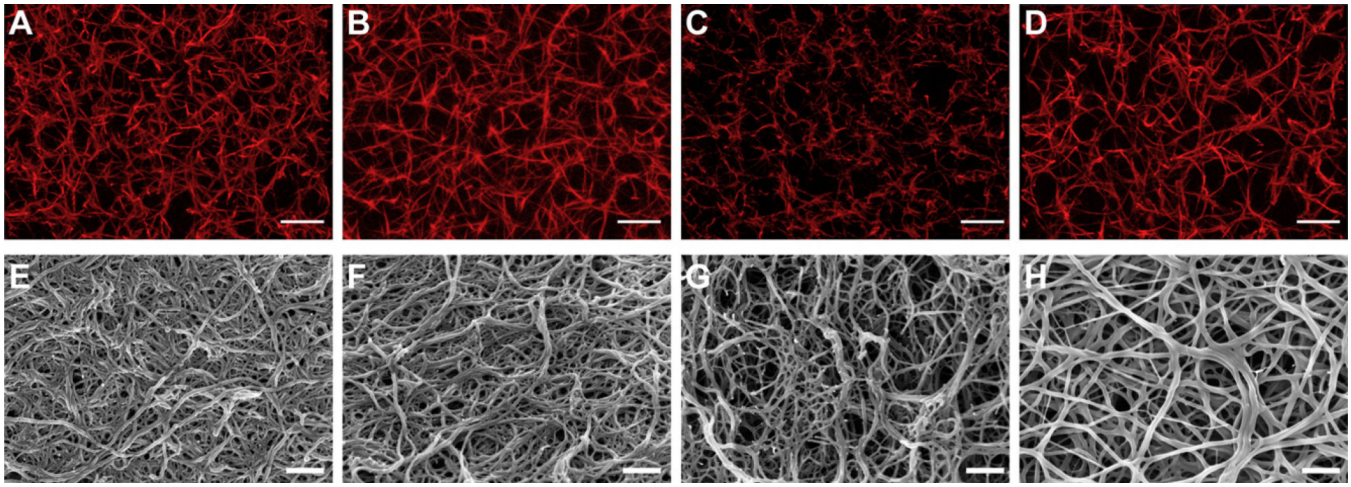

Fig. 2.

Confocal and scanning electron microscopy: Representative confocal micrograph projections (10 μm z-stacks; A–D) and SEM images (E–H) from no peptide control (A and E), control peptide conjugate, GPSPFPAC-PEG (B and F), knob 'A' conjugate, GPRPFPAC-PEG (C and G), and knob 'B' conjugate, AHRPYAAC-PEG (D and H). Confocal: Objective = 63×, Scale bar = 10 μm. SEM: Magnification = 50,000×, Voltage = 3.0 kV, Scale bar = 500 nm.

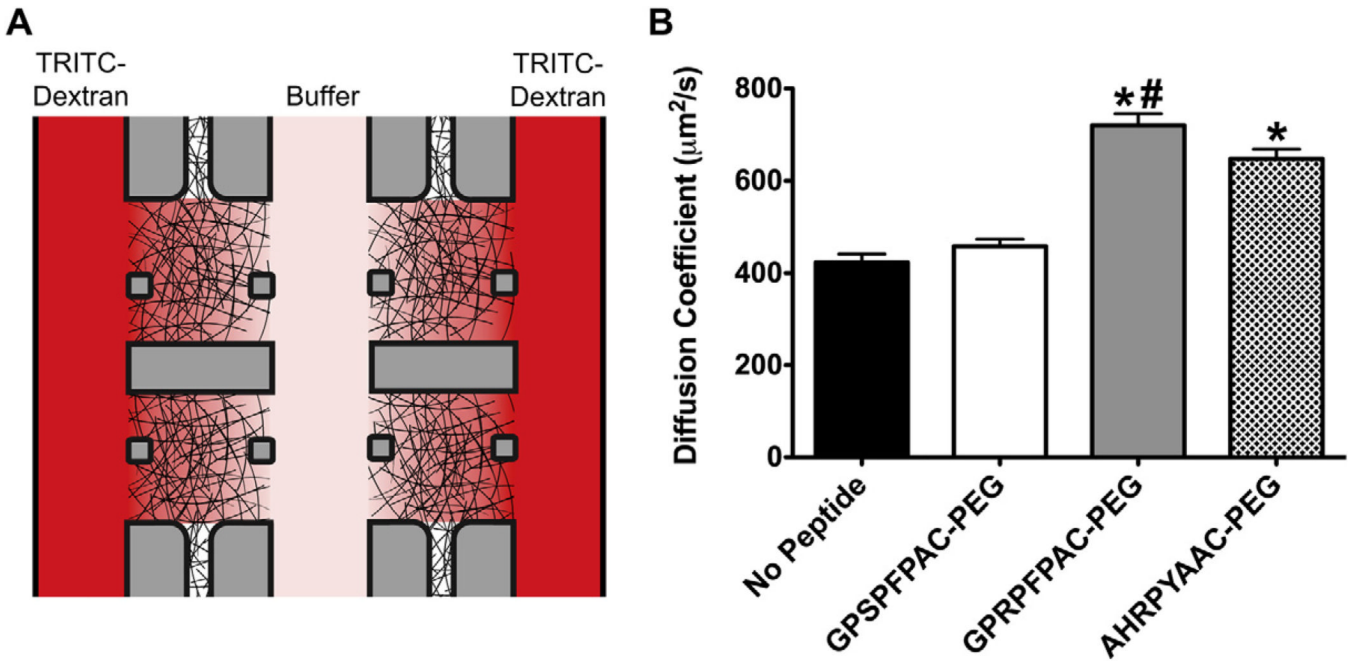

Fig. 3.

Effective diffusion coefficient: Schematic of microfluidic devise used to track diffusion of fluorescently labeled dextran through fibrin gels (A). Diffusion coefficient as measured within a 4 mg/mL fibrinogen gel supplemented with fibrin knob conjugates (B). (Mean ± SD; $n = 4$; * denotes $p < 0.001$ relative to all groups, # denotes $p < 0.01$ relative to AHRPYAAC-PEG).

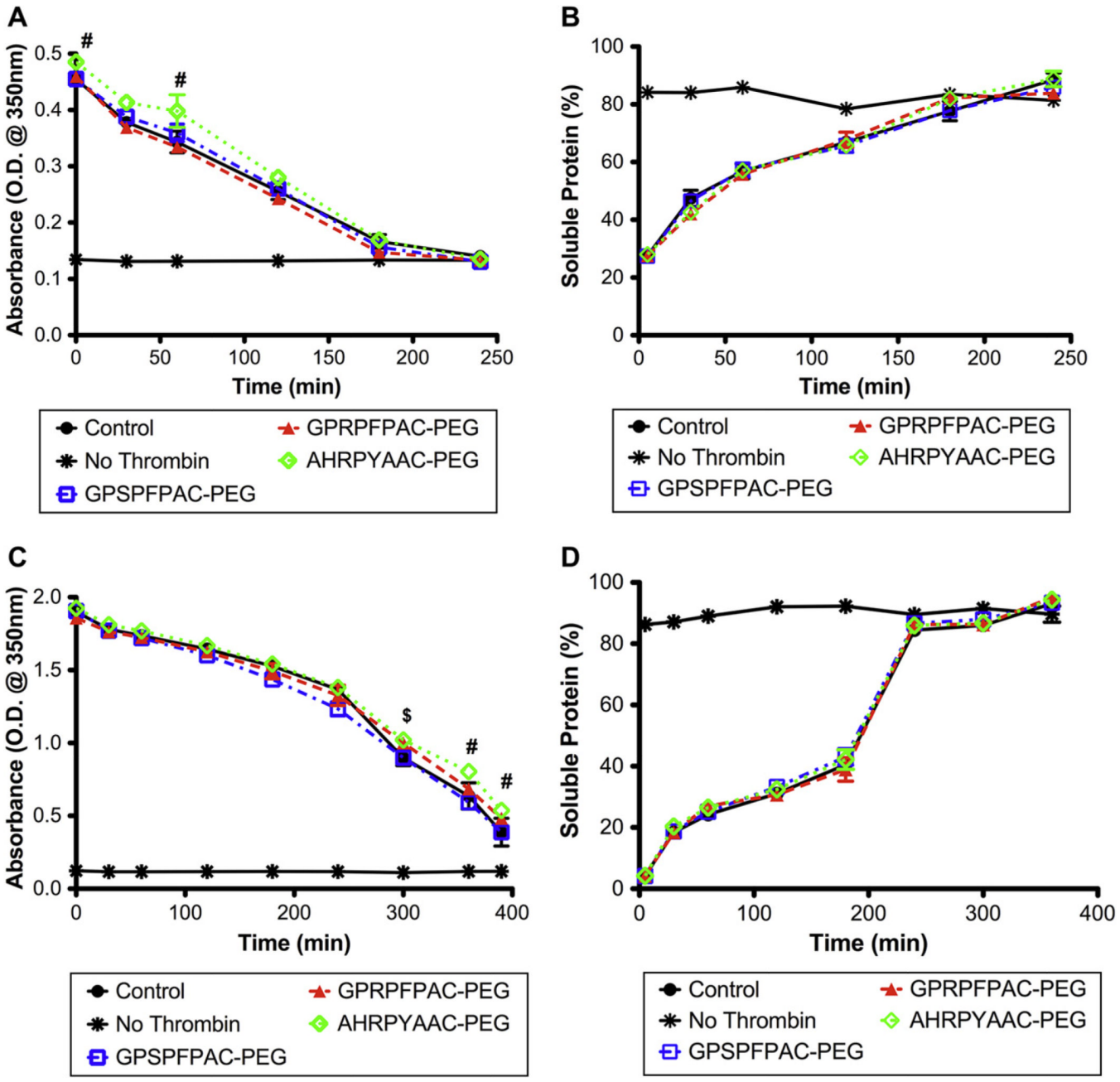

Fig. 4.

Exogenous fibrinolysis: Fibrinolysis of pre-formed fibrin clots of 1 mg/mL fibrinogen (A, B) or 4 mg/mL fibrinogen (C, D). Absorbance measurements at 350 nm (A, C) and soluble protein (B, D) were used to follow lysis progression. No peptide control (●), No thrombin control (❋), Control peptide, GPSPFPAC-PEG (□), knob 'A' conjugate, GPRPFPAC-PEG (△), knob 'B' conjugate, AHRPYAAC-PEG (◇). (Mean ± SD; $n = 4$; # denotes $p < 0.01$ relative to all groups, $ denotes $p < 0.01$ relative to GPRPFPAC-PEG).

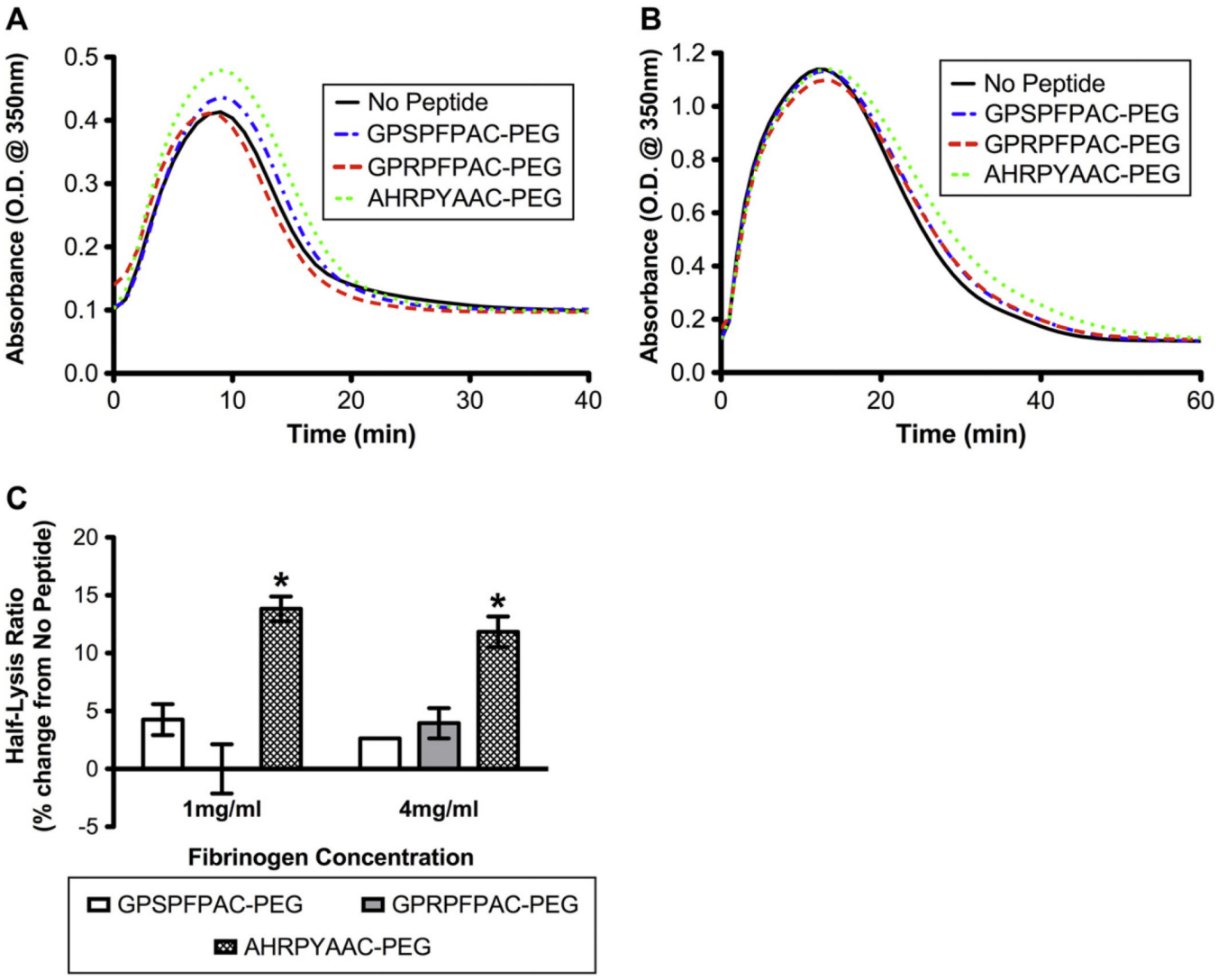

Fig. 5.

Endogenous fibrinolysis: Absorbance measurements at 350 nm for plasminogen/tPA stimulated fibrinolysis of fibrin with 1 mg/mL fibrinogen (A) or 4 mg/mL fibrinogen (B). Half-lysis ratio relative to no peptide control (C). (Mean ± SD; $n = 6$; # denotes $p < 0.01$ relative to all groups).

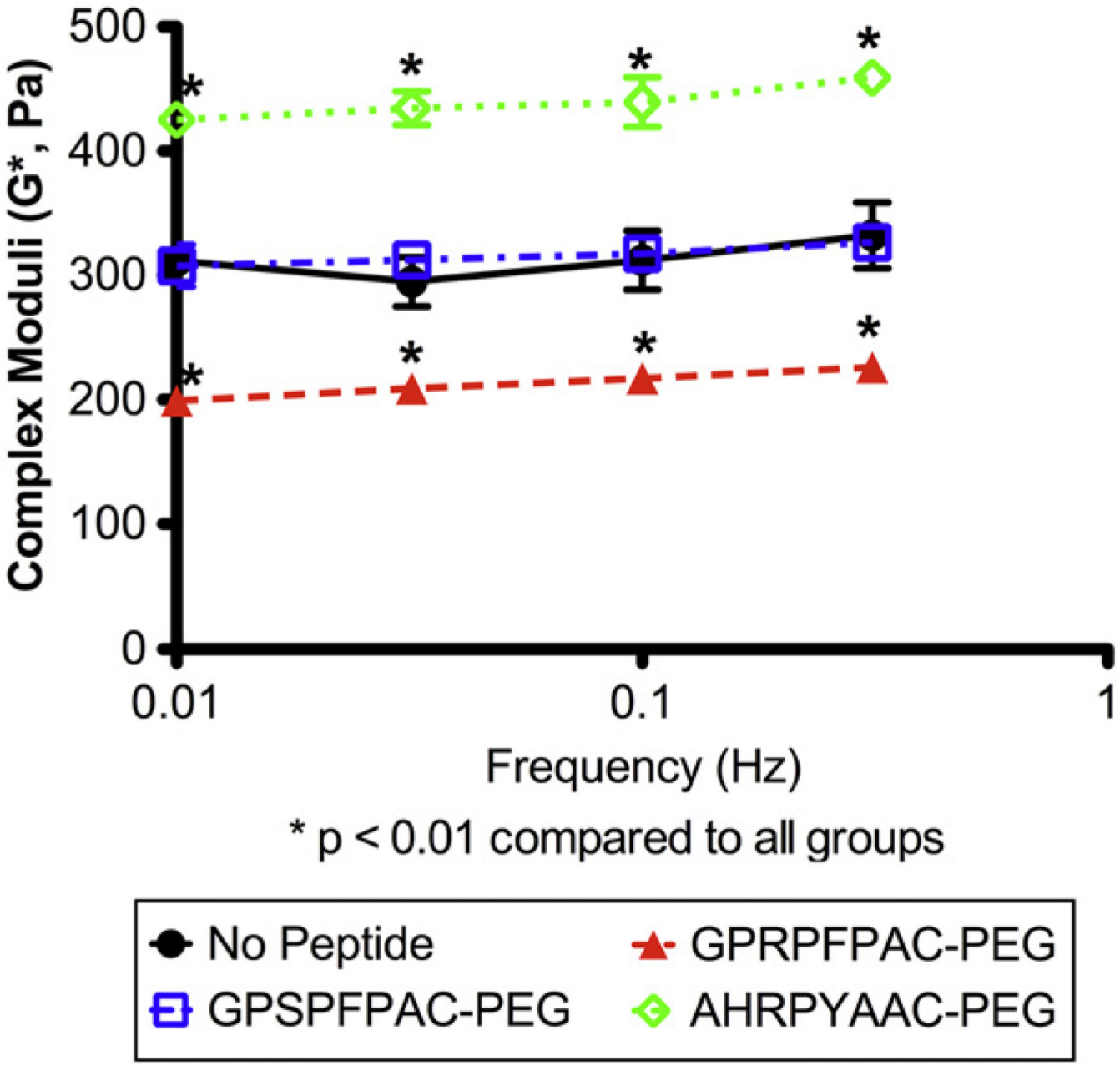

Fig. 6.

Viscoelasticity: Complex moduli (G*) for 4 mg/mL fibrinogen gels supplemented with or without fibrin knob peptide conjugates. No peptide control (●), Control peptide, GPSPFPAC-PEG (□), knob 'A' conjugate, GPRPFPAC-PEG (▲), knob 'B' conjugate, AHRPYAAC-PEG (◇). (Mean ± SD; $n = 4$; # denotes $p < 0.01$ relative to all groups).

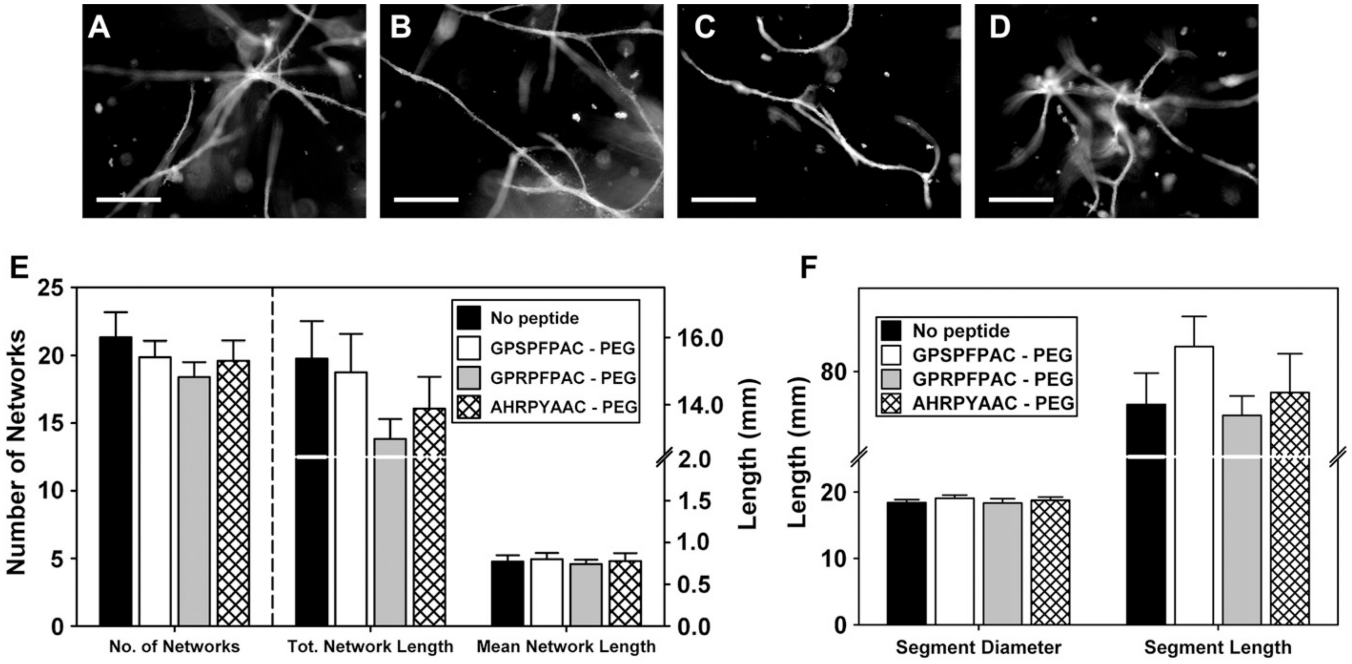

Fig. 7.

Angiogenic sprouting from microvessel fragments: Representative fluorescence micrographs of constructs at day 10 from no peptide control (A), control peptide (GPSPFPAC-PEG; B), knob 'A' conjugate (GPRPFPAC-PEG; C), and knob 'B' conjugate (AHRPYAAC; D). Scale bar = 200 μm. Comparison of network characteristics across the substrates (E), Comparison of segment characteristics across the substrates (F). Note that multiple connected segments are contained within a network. No significant difference was observed between groups.